Letter

Intrinsically interacting higher-order topological superconductors

Hao-Ran Zhang,[1,*] Jian-Hao Zhang,[2,3,*] Zheng-Cheng Gu,[2,†] Rui-Xing Zhang,[4,5,6,‡] and Shuo Yang[1,7,8,§]

[1]*State Key Laboratory of Low Dimensional Quantum Physics and Department of Physics, Tsinghua University, Beijing 100084, China*
[2]*Department of Physics, The Chinese University of Hong Kong, Shatin, New Territory, Hong Kong, China*
[3]*Department of Physics, The Pennsylvania State University, University Park, Pennsylvania 16802, USA*
[4]*Department of Physics and Astronomy, The University of Tennessee, Knoxville, Tennessee 37996, USA*
[5]*Department of Materials Science and Engineering, The University of Tennessee, Knoxville, Tennessee 37996, USA*
[6]*Institute for Advanced Materials and Manufacturing, The University of Tennessee, Knoxville, Tennessee 37920, USA*
[7]*Frontier Science Center for Quantum Information, Beijing 100084, China*
[8]*Hefei National Laboratory, Hefei 230088, China*

(Received 9 January 2023; revised 30 June 2023; accepted 24 July 2023; published 11 August 2023)

We propose a minimal interacting lattice model for two-dimensional class-D higher-order topological superconductors with no free-fermion counterpart. A Lieb-Schultz-Mattis-type constraint has been proposed and applied to guide our lattice model construction. Our model exhibits a trivial product ground state in the weakly interacting regime, whereas, increasing electron correlations provoke a novel topological quantum phase transition to a D_4-symmetric higher-order topological superconducting state. The symmetry-protected Majorana corner modes are numerically confirmed with the matrix-product-state technique. Our theory paves the way for studying correlated higher-order topology with explicit lattice model constructions.

DOI: 10.1103/PhysRevB.108.L060504

Introduction. The discovery of the quantum Hall effect [1,2] raised the curtain on one of the greatest triumphs of condensed-matter physics, the topological phases of matter. Different from traditional Landau's paradigm, phases with topological distinctions are characterized by their patterns of long-range entanglement rather than symmetry-breaking orders. Moreover, lattice or internal symmetries can help short-range entangled states develop additional topological structures, leading to symmetry-protected topological (SPT) phases [3–26]. Recently, SPT phases protected by crystalline symmetries have been under the research spotlight [5,27–60], mainly attributed to their capability of supporting an exotic *higher-order* topological bulk-boundary correspondence. Namely, an nth order topological phenomenon takes place when $(d-n)D$ gapless boundary modes $(1 < n \leqslant d)$ show up in a dD crystalline SPT phase [61–79]. In particular, a two-dimensional (2D) higher-order topological superconductor (HOTSC) will, by definition, host non-Abelian Majorana modes that reside around the sample geometric corners, and recent studies have proposed schemes to realize the non-Abelian braiding of Majorana corner modes [80,81], which offers a new platform to topologically encode quantum information.

The state-of-the-art development of topological band theory phrased as *symmetry indicators* [82–85] has boosted our understanding of HOTSCs at the free-fermion level with a plethora of candidate systems having been theoretically proposed. Nonetheless, no convincing experimental evidence of HOTSC physics has been reported, thus far. Although the symmetry indicator theory only applies to free-fermion systems, the formation of HOTSC usually requires an unconventional pairing symmetry, which likely arises from electron interaction effects. Therefore, a faithful microscopic theory or prediction of HOTSC would also require comprehensive knowledge of relevant topological physics in the strongly interacting regime. Along this direction, recent works have established a constructive classification scheme of crystalline fermion SPT phases (e.g., Refs. [43,44,51,60]), which involves novel topological structures that can be interpreted as interacting HOTSC phases with no free-fermion counterpart. However, the real-space constructions in the classification are relatively abstract, leaving it unclear whether and how these new and exciting ideas of *intrinsically* interacting HOTSCs can be modeled in a concrete lattice system, let alone realized in a laboratory. This motivates us to design explicit lattice models to realize these exotic phases. With the explicit lattice model, hopefully it will become more possible to explore this intrinsically interacting HOTSC physics in experiments and facilitate the development of Majorana-based quantum computation.

In this Letter, we construct a minimal lattice model of 2D HOTSC that cannot be realized in any free-fermion systems. The SPT nature of our model is supported by a Lieb-Schultz-Mattis-type (LSM-type) constraint, the original version of which forbids a unique gapped symmetric ground state in a one-dimensional (1D) spin-1/2 chain with translation symmetry and SO(3) on-site symmetry [86], and can be generalized to higher dimensions and other internal

*These authors contributed equally to this work.
†zcgu@phy.cuhk.edu.hk
‡ruixing@utk.edu
§shuoyang@tsinghua.edu.cn

symmetries [87–89]. The LSM-type constraint can be viewed as the certain bulk-boundary correspondence of weak SPT phase in one higher dimension, or, alternatively, can be interpreted as a mixed anomaly between translation symmetry and internal symmetry [56,57]. The LSM-type theorem reveals that the microscopic structure of a lattice system can impose strong constraints on its low-energy behavior. It, therefore, serves as a useful criterion to help us exclude lattice constructions that are SPT impossible (i.e., forbid a unique gapped symmetric ground state) and further guides us to the "correct" lattice models with desired topological properties. Building upon this starting point, we begin with a free-fermion Hamiltonian in a designed lattice and add proper D_4-symmetric interactions to it. In the absence of interactions, our model exhibits a trivial gapped phase, which persists when moderate interactions are turned on. Further increasing the interaction strength triggers a novel topological quantum phase transition between the trivial phase and the HOTSC phase, the critical behavior of which has been carefully studied here. We also confirm the signature Majorana corner modes of the HOTSC phase numerically by placing our model on an open-boundary two-leg ladder geometry with the help of the matrix-product-state (MPS) technique. Our lattice model is an important step towards bridging the gap between the formal classification theory and the materialization of strongly interacting higher-order topological physics.

LSM-type constraint. The LSM-type constraint was originally proposed in 1D spin systems with translation symmetry and later generalized to 2D translationally invariant systems with various internal symmetries [86–89]. It is natural to generalize the LSM-type constraint to systems with general crystalline symmetry. However, there is a significant difference between crystalline symmetry and internal symmetry. In systems with crystalline symmetry, the effective on-site symmetry, often known as a *site symmetry group* [90], can vary across different spatial locations. One may simplify this situation by placing physical degrees of freedom only on the maximal Wyckoff positions of the lattice. This simplification is supported by the fact that physical degrees of freedom if not being maximally Wyckoff positioned can always be smoothly deformed to these maximal Wyckoff positions symmetrically through a lattice homotopy [91]. As a result, the LSM-type constraint for crystalline-symmetric lattice systems should be defined for the maximal Wyckoff positions.

The LSM-type constraint for topological crystalline phases in 2D interacting fermionic systems is defined as a gapped nondegenerate ground state requires that the system can be adiabatically connected to a state with an integer multiple of linear representations of the total symmetry group at maximal Wyckoff positions per unit cell [92]. In other words, if the physical degrees of freedom within a unit cell can be deformed to a projective representation of the total symmetry group at maximal Wyckoff positions, the ground state either breaks symmetry or has gapless excitations. In Supplemental Material, we demonstrate the LSM-type constraint in 2D fermionic systems with D_2 symmetry [92]. A lattice system that satisfies the LSM-type constraint forbids a unique gapped symmetric ground state, and, thus, cannot be a candidate for SPT phase. As a result, the LSM-type constraint immensely reduces the possibilities of assigning physical degrees of freedom on the lattice and greatly simplifies the model construction of the higher-order crystalline topological phase.

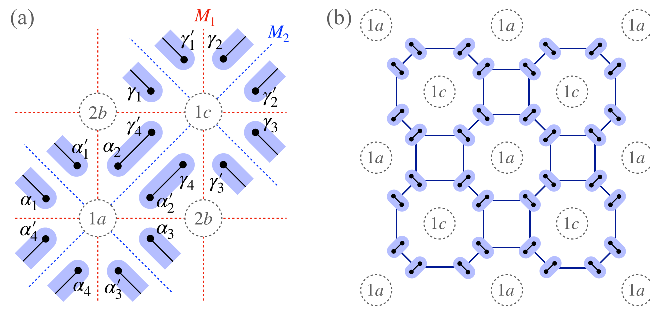

FIG. 1. (a) Reflection generators $\boldsymbol{M}_{1,2}$ and maximal Wyckoff positions (dashed circles) a, b, c of D_4. Blue shadows depict atomic sites assigned between each neighboring maximal Wyckoff positions a and c, composed of two Majorana zero modes depicted by two solid dots. (b) Lattice in the open boundary condition, where $1a/1c$ denotes the maximal Wyckoff position. Atomic sites are placed on a square-octagon lattice depicted by solid lines.

D_4-symmetric HOTSC. Now, we apply the LSM-type constraint to a system with D_4-crystalline symmetry. The fourfold dihedral group D_4 is the semidirect product of a fourfold rotation group C_4 and a reflection group $\mathbb{Z}_2^M$ (i.e., $D_4 = C_4 \rtimes \mathbb{Z}_2^M$). Alternatively, as illustrated in Fig. 1(a), D_4 can be generated by two reflection operators $\boldsymbol{M}_1$ and $\boldsymbol{M}_2$. There are three maximal Wyckoff positions per unit cell, denoted as $\boldsymbol{q}_a = (0, 0)$, $\boldsymbol{q}_b = (0, 1/2)$, or $(1/2, 0)$ and $\boldsymbol{q}_c = (1/2, 1/2)$. Here, the site-symmetry group for both a and c is D_4, whereas, that for b is D_2. To build a D_4-symmetric 2D HOTSC with a unique gapped ground state, the LSM-type constraint requires an even number of (pseudo) spin-1/2 degrees of freedom at maximal Wyckoff positions per unit cell because a spin-1/2 degree of freedom forms a projective representation of a D_4 group. Note that a pair of spinless fermions, or equivalently, four Majorana fermions, can form a spin-1/2 operator. Thus, we should place, at least, eight Majorana operators at each occupied maximal Wyckoff position for a gapped SPT state to emerge.

Following that, we consider a lattice model with 16 Majorana operators per unit cell, eight at each maximal Wyckoff position a/c, which form a linear representation of $\mathbb{Z}_2^f \times D_4$. As shown in Fig. 1(a), we label these Majorana fermions α_k, α'_k, γ_k, and γ'_k, with $k = 1, 2, 3, 4$. To describe a physical superconductor, the Majorana fermions must come in pairs to form complex fermions corresponding to atomic sites (denoted by the blue shadows), which sit around the midpoints between Wyckoff positions a and c. As shown in Fig. 1(b), the complex fermions together form a square-octagon lattice. We construct a D_4-symmetric Hamiltonian with intraite Majorana pairs denoted by the black solid lines in Fig. 1(a),

$$H_0 = it \sum_j (\alpha_{2,j}\gamma'_{4,j} + \alpha'_{2,j}\gamma_{4,j} + \alpha_{3,j}\gamma'_{1,j-\hat{y}} + \alpha'_{3,j}\gamma_{1,j-\hat{y}} + \alpha_{4,j}\gamma'_{2,j-\hat{x}-\hat{y}} + \alpha'_{4,j}\gamma_{2,j-\hat{x}-\hat{y}} + \alpha_{1,j}\gamma'_{3,j-\hat{x}} + \alpha'_{1,j}\gamma_{3,j-\hat{x}}). \quad (1)$$

The additional subscript j of the Majorana operator labels the unit cell. One can easily verify that H_0 is invariant under D_4 action via the following symmetry transformations:

$$\boldsymbol{M}_1\colon \begin{matrix}(\alpha_1,\alpha_2,\alpha_3,\alpha_4)\leftrightarrow(\alpha_2',\alpha_1',\alpha_4',\alpha_3')\\(\gamma_1,\gamma_2,\gamma_3,\gamma_4)\leftrightarrow(\gamma_2',\gamma_1',\gamma_4',\gamma_3')\end{matrix}$$
$$\boldsymbol{M}_2\colon \begin{matrix}(\alpha_1,\alpha_2,\alpha_3,\alpha_4)\leftrightarrow(\alpha_3',\alpha_2',\alpha_1',\alpha_4')\\(\gamma_1,\gamma_2,\gamma_3,\gamma_4)\leftrightarrow(\gamma_3',\gamma_2',\gamma_1',\gamma_4').\end{matrix} \quad (2)$$

Here, we omit the subscript j for simplicity. For Majorana modes away from the symcenter, their subscripts j should transform accordingly.

In this way, the Majorana pairs in Eq. (1) are local mass terms of complex fermions. Therefore, the ground state of H_0 is clearly a topologically trivial product state. In fact, one can show that a free-fermion lattice model respecting the same set of lattice symmetries must always be topologically trivial [44].

Towards a nontrivial HOTSC, there should be intersite couplings centered at the maximal Wyckoff positions. Due to the crystalline symmetry constraint, the pairing between two Majoranas on the different sides of the reflection axis is forbidden since the reflection will inverse the direction of pairing. Hence, the intersite couplings need to be some four-fermion interaction. Thus, we now explore the topological consequence of four-fermion interactions in our model. The interacting Hamiltonian should be D_4 symmetric and trivially gapped in the periodic boundary conditions (PBC). For the sake of convenience, at each maximal Wyckoff position a or c, we redefine four complex fermion operators from Majorana operators ($k = 1, 2, 3, 4$),

$$\begin{aligned}c_{k,ja}^{\dagger} &= \tfrac{1}{2}(\alpha_{k,j}+i\alpha_{k,j}')\\ c_{k,jc}^{\dagger} &= \tfrac{1}{2}(\gamma_{k,j}+i\gamma_{k,j}').\end{aligned} \quad (3)$$

This redefinition of complex fermions is equivalent to a change in basis or unitary transformation in the Hilbert space. The particle number operators of these complex fermions are denoted as $n_{k,ja} = c_{k,ja}^{\dagger}c_{k,ja}$ and $n_{k,jc} = c_{k,jc}^{\dagger}c_{k,jc}$. We first introduce Hubbard interactions H_U for these complex fermions, which are D_4-symmetric ($U > 0$),

$$H_U = U\sum_j\sum_{s=a,c}\sum_{k=1}^{2}\left(n_{k,js}-\frac{1}{2}\right)\left(n_{k+2,js}-\frac{1}{2}\right). \quad (4)$$

In PBC, all Majorana operators are involved in H_U, and the occupations result in a fourfold ground state degeneracy (GSD) per a/c site, i.e., $(n_{1,js}, n_{3,js})$ or $(n_{2,js}, n_{4,js}) = (0, 1)$ or (1,0). This fourfold GSD can be effectively regarded as two pseudo-spin-1/2 degrees of freedom per site,

$$\begin{aligned}\tau_{13,js}^{\mu} &= (c_{1,js}^{\dagger}, c_{3,js}^{\dagger})\sigma^{\mu}\begin{pmatrix}c_{1,js}\\c_{3,js}\end{pmatrix},\\ \tau_{24,js}^{\mu} &= (c_{2,js}^{\dagger}, c_{4,js}^{\dagger})\sigma^{\mu}\begin{pmatrix}c_{2,js}\\c_{4,js}\end{pmatrix}, \quad s=a,c.\end{aligned} \quad (5)$$

where σ^x, σ^y, and σ^z are Pauli matrices. Then, we introduce a spin-spin interaction at each maximal Wyckoff position ($J > 0$),

$$H_J = J\sum_j[\boldsymbol{\tau}_{13,ja}*\boldsymbol{\tau}_{24,ja}+\boldsymbol{\tau}_{13,jc}*\boldsymbol{\tau}_{24,jc}]. \quad (6)$$

Here, $*$ is defined as $\boldsymbol{S}_1 * \boldsymbol{S}_2 = S_1^xS_2^x + S_1^yS_2^z - S_1^zS_2^y$ to satisfy D_4 symmetry Eq. (2). H_J lifts the GSD of H_U to a nondegenerate ground state, which is a spin-singlet assembly. Note that when viewed on the previous basis (corresponding to real atomic sites), this ground state is not a product state because the alternative complex fermions defined in Eq. (3) are virtual and cannot be gapped by local mass terms. At each maximal Wyckoff position a or c, the nondegenerate ground state in the pseudospin basis is

$$|\psi\rangle = \tfrac{1}{2}(|\uparrow,\uparrow\rangle + i|\uparrow,\downarrow\rangle - i|\downarrow,\uparrow\rangle - |\downarrow,\downarrow\rangle). \quad (7)$$

Likewise, each maximal Wyckoff position a/c carries a linear representation. According to the LSM-type constraint, the interaction terms $H_U + H_J$ at each maximal Wyckoff position are suitable candidates for constructing a 2D HOTSC.

Following that, we investigate the topological properties of the proposed model in the topological nontrivial ($U/t \gg 1$) regime. We will see that Majorana zero modes appear at the geometric corners of the system in the open boundary condition (OBC) as a signature of the HOTSC phase. As shown in Fig. 1(b), for the lattice in OBC, all Majorana modes in the bulk are gapped out by $H_U + H_J$, whereas, Majorana modes on the boundary are not involved in interaction terms, resulting in gapless dangling boundary modes. Those 1D gapless boundary modes can be gapped out by a D_4-symmetric perturbation,

$$\begin{aligned}H' = \epsilon\sum_j(&\alpha_{1,j}\alpha_{1,j}'\alpha_{2,j}\alpha_{2,j}' + \alpha_{2,j}\alpha_{2,j}'\alpha_{3,j}\alpha_{3,j}'\\ &+ \alpha_{3,j}\alpha_{3,j}'\alpha_{4,j}\alpha_{4,j}' + \alpha_{4,j}\alpha_{4,j}'\alpha_{1,j}\alpha_{1,j}').\end{aligned} \quad (8)$$

The remaining zero-dimensional gapless boundary modes η_k and η_k' ($k = 1, 2, 3, 4$) are all strictly localized at the corner of the system [see Fig. 2(a)] with two at each corner and the symmetry properties,

$$\begin{aligned}&\boldsymbol{M}_1\colon \begin{cases}(\eta_1,\eta_4)\leftrightarrow(\eta_2,\eta_3),\\(\eta_1',\eta_4')\leftrightarrow(\eta_2',\eta_3'),\end{cases}\\ &\boldsymbol{M}_2\colon (\eta_1,\eta_2,\eta_3,\eta_4)\leftrightarrow(\eta_3',\eta_2',\eta_1',\eta_4').\end{aligned} \quad (9)$$

These eight Majorana zero modes are protected by D_4 symmetry and cannot be gapped out by symmetric perturbations. The only possible way to gap out is to introduce a Majorana pair at each corner $i\eta_j\eta_j'$ ($j = 1, 2, 3, 4$). However, these terms break the reflection operation in D_4 symmetry either diagonally or off diagonally [see dashed lines in Fig. 2(a)], e.g., $\boldsymbol{M}_2\colon i\eta_2\eta_2' \to -i\eta_2\eta_2'$. As a result, all these Majorana corner modes are robust against D_4-symmetric perturbations, which feature a HOTSC phase.

We now numerically investigate the general case of our model with $t, U, J \neq 0$, and verify the Majorana corner modes of the HOTSC phase in the strongly interacting regime. Consider the interacting Hamiltonian $H = H_0 + H_U + H_J$ on a 2×20 two-leg ladder geometry with OBC in the horizontal direction and PBC in the vertical direction. The computational

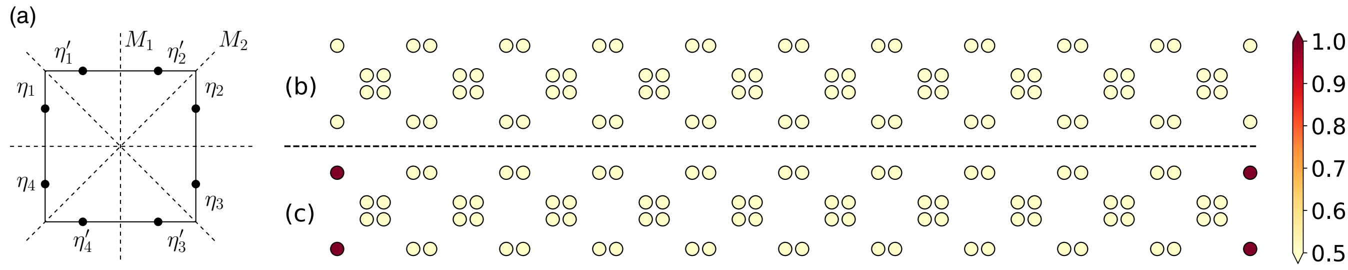

FIG. 2. (a) Sketch of Majorana zero modes of D_4-symmetric HOTSC at geometric corners in OBC. (b) and (c) Evolution of Majorana corner modes of the Hamiltonian $H = H_0 + H_U + H_J$ on a two-leg ladder when slightly tuned away from half-filling from (b) weakly interacting regime with $t = 1,\ U = J = 0.1$ to (c) strongly interacting regime with $t = 1,\ U = J = 10$. The color of each point indicates the ground-state density expectation value of complex fermions defined in Eq. (3).

basis is taken as the Fock basis with complex fermion operators defined as Eq. (3). H represents a half-filling system on this basis, and the electron density for the ground state is exactly $n_i = 0.5$ at each site. Because H is fully gapped in the bulk, perturbing H with a small chemical potential μ allows us to reveal the zero modes. When μ slightly deviates from 0, the variation of n_i from half-filling reveals the density distribution of zero modes. The density distribution with $\mu = 0.2$ for both the weakly interacting regime and the strongly interacting regime is plotted in Fig. 2. In the weakly interacting regime [Fig. 2(b)], μ induces hardly any density variation, showing that there is no gapless edge mode and the phase is trivial. In the strongly interacting regime [Fig. 2(c)], however, an obvious density variation occurs, which is strictly localized at the corners. This demonstrates the existence of Majorana corner modes as well as the HOTSC phase. The numerical result is consistent with our previous analysis in the free limit ($U, J \to 0$) and strong interaction limit ($t \to 0$). The robustness of the Majorana corner modes against D_4-symmetric perturbations reveals the nontrivial topology of the model we have constructed. We emphasize that such a nontrivial topological property is a result of strong electron interactions.

Furthermore, we find a topological quantum phase transition (QPT) by tuning the ratio of interaction strength to the intensity of Majorana pairs U/t. As previously stated, the system is a trivial product state when $U/t \ll 1$, whereas, it is a 2D D_4-symmetry-protected HOTSC when $U/t \gg 1$. This QPT is characterized by the divergence of the correlation length ξ on an infinite-length two-leg ladder, which is determined by the ratio between the two largest eigenvalues of the MPS transfer matrix [93]. We fix $t = 1$ on a $2 \times \infty$ lattice, tune the interaction strength U ($J = U$), and calculate ξ for various U's ranging from 0 to 8 as shown in Fig. 3. ξ diverges at $U_c \sim 1.038$, implying an unambiguous topological QPT between a trivial product state and an extended HOTSC. As shown in the inset of Fig. 3, the correlation length exhibits a perfect power-law divergence for $U \lesssim U_c$, and we fit the critical exponent $\xi \propto |U - U_c|^{-0.40}$. This QPT is also implied by the evolutions of Majorana corner modes for various U/t ratios as shown in Fig. 2. According to the classification of 2D crystalline fermionic SPT phases in Ref. [44], the lattice model we constructed in this Letter is the only possible 2D intrinsically interacting class-D HOTSC, for both spinless and spin-1/2 fermions.

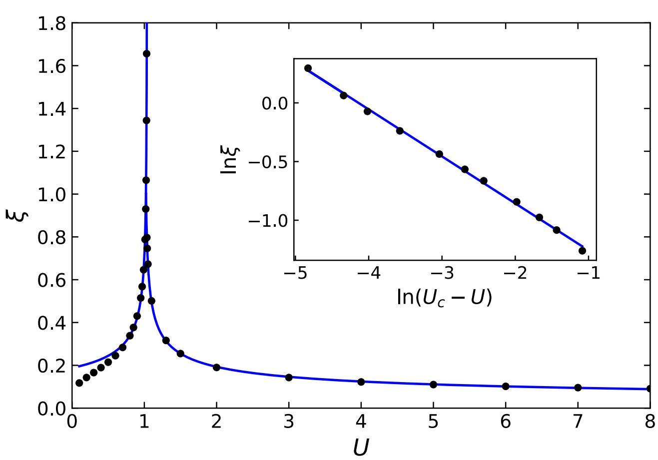

FIG. 3. The correlation lengths ξ of the matrix product state as a function of U with fixed $t = 1$ and $J = U$. The power-law divergence of ξ near the critical point $U_c \sim 1.038$ signifies a quantum phase transition.

Conclusion and discussion. In this Letter, we construct an intrinsically interacting lattice model of 2D D_4-symmetric class-D HOTSC using the LSM-type constraint. An indispensable advantage of the LSM-type constraint is that it considerably simplifies the lattice model construction: only physical degrees of freedom forming linear representations of the total symmetry group at maximal Wyckoff positions are allowed. With the concrete lattice model, we study its Majorana corner modes, which are robust under symmetric perturbations, and find that there are two Majorana zero modes at each corner of the system. Subsequently, we perform MPS calculations on systems with two-leg ladder geometry in order to tackle the general interacting Hamiltonian. We see the stability of Majorana corner modes and find an unambiguous topological QPT between a 2D HOTSC and a trivial product state, controlled by the ratio between the intensity of interactions and Majorana pairs. The concrete lattice model we developed here is the only possible 2D intrinsically interacting class-D HOTSC, and explicit and robust Majorana corner modes are experimentally relevant and can be directly measured with spectroscopic experiments on monolayer iron-selenide (FeSe, a strongly correlated material whose point-group symmetry is D_4). Lattice model construction with the LSM-type constraint established in this Letter can be generalized to systems with any dimension and any spatial or internal symmetry for interacting fermionic systems.

Acknowledgments. Stimulating discussions with Z. Bi and M. Cheng are acknowledged. H.-R.Z. and S.Y. are supported by the National Natural Science Foundation of China (NSFC) (Grants No. 12174214 and No. 92065205), the National Key R&D Program of China (Grant No. 2018YFA0306504), and the Innovation Program for Quantum Science and Technology (Grant No. 2021ZD0302100). J.-H.Z. and Z.-C.G. were supported by Direct Grant No. 4053462 from The Chinese University of Hong Kong and funding from Hong Kongs Research Grants Council (Grant No. 14307621, ANR/RGC Joint Research Scheme No. A-CUHK402/18). R.-X.Z. was supported by a startup fund at the University of Tennessee.

[1] D. C. Tsui, H. L. Stormer, and A. C. Gossard, Two-Dimensional Magnetotransport in the Extreme Quantum Limit, Phys. Rev. Lett. **48**, 1559 (1982).
[2] R. B. Laughlin, Anomalous Quantum Hall Effect: An Incompressible Quantum Fluid with Fractionally Charged Excitations, Phys. Rev. Lett. **50**, 1395 (1983).
[3] Z.-C. Gu and X.-G. Wen, Tensor-entanglement-filtering renormalization approach and symmetry-protected topological order, Phys. Rev. B **80**, 155131 (2009).
[4] X. Chen, Z.-C. Gu, and X.-G. Wen, Classification of gapped symmetric phases in one-dimensional spin systems, Phys. Rev. B **83**, 035107 (2011).
[5] H. C. Po, A. Vishwanath, and H. Watanabe, Symmetry-based indicators of band topology in the 230 space groups, Nat. Commun. **8**, 50 (2017).
[6] X. Chen, Z.-C. Gu, Z.-X. Liu, and X.-G. Wen, Symmetry-protected topological orders in interacting bosonic systems, Science **338**, 1604 (2012).
[7] X. Chen, Z.-C. Gu, Z.-X. Liu, and X.-G. Wen, Symmetry protected topological orders and the group cohomology of their symmetry group, Phys. Rev. B **87**, 155114 (2013).
[8] T. Senthil, Symmetry-protected topological phases of quantum matter, Annu. Rev. Condens. Matter Phys. **6**, 299 (2015).
[9] E. Plamadeala, M. Mulligan, and C. Nayak, Short-range entangled bosonic states with chiral edge modes and t duality of heterotic strings, Phys. Rev. B **88**, 045131 (2013).
[10] Y.-M. Lu and A. Vishwanath, Theory and classification of interacting integer topological phases in two dimensions: A chern-simons approach, Phys. Rev. B **86**, 125119 (2012).
[11] D. S. Freed, Short-range entanglement and invertible field theories, arXiv:1406.7278.
[12] D. S. Freed and M. J. Hopkins, Reflection positivity and invertible topological phases, Geom. Topol. **25**, 1165 (2021).
[13] Z.-C. Gu and X.-G. Wen, Symmetry-protected topological orders for interacting fermions: Fermionic topological nonlinear σ models and a special group supercohomology theory, Phys. Rev. B **90**, 115141 (2014).
[14] Q.-R. Wang and Z.-C. Gu, Towards a Complete Classification of Symmetry-Protected Topological Phases for Interacting Fermions in Three Dimensions and a General Group Supercohomology Theory, Phys. Rev. X **8**, 011055 (2018).
[15] Q.-R. Wang and Z.-C. Gu, Construction and Classification of Symmetry-Protected Topological Phases in Interacting Fermion Systems, Phys. Rev. X **10**, 031055 (2020).
[16] A. Kapustin, Symmetry protected topological phases, anomalies, and cobordisms: Beyond group cohomology, arXiv:1403.1467.
[17] A. Kapustin, R. Thorngren, A. Turzillo, and Z. Wang, Fermionic symmetry protected topological phases and cobordisms, J. High Energy Phys. 12 (2015) 052.
[18] A. Kapustin and R. Thorngren, Fermionic spt phases in higher dimensions and bosonization, J. High Energy Phys. 10 (2017) 080.
[19] Z.-C. Gu and M. Levin, Effect of interactions on two-dimensional fermionic symmetry-protected topological phases with z_2 symmetry, Phys. Rev. B **89**, 201113(R) (2014).
[20] M. Cheng and Z.-C. Gu, Topological Response Theory of Abelian Symmetry-Protected Topological Phases in Two Dimensions, Phys. Rev. Lett. **112**, 141602 (2014).
[21] M. Barkeshli, P. Bonderson, M. Cheng, and Z. Wang, Symmetry fractionalization, defects, and gauging of topological phases, Phys. Rev. B **100**, 115147 (2019).
[22] N. Tantivasadakarn, Dimensional reduction and topological invariants of symmetry-protected topological phases, Phys. Rev. B **96**, 195101 (2017).
[23] C. Wang, C.-H. Lin, and Z.-C. Gu, Interacting fermionic symmetry-protected topological phases in two dimensions, Phys. Rev. B **95**, 195147 (2017).
[24] M. Cheng, Z. Bi, Y.-Z. You, and Z.-C. Gu, Classification of symmetry-protected phases for interacting fermions in two dimensions, Phys. Rev. B **97**, 205109 (2018).
[25] M. Cheng, N. Tantivasadakarn, and C. Wang, Loop Braiding Statistics and Interacting Fermionic Symmetry-Protected Topological Phases in Three Dimensions, Phys. Rev. X **8**, 011054 (2018).
[26] S.-Q. Ning, C. Wang, Q.-R. Wang, and Z.-C. Gu, Edge theories of two-dimensional fermionic symmetry protected topological phases protected by unitary abelian symmetries, Phys. Rev. B **104**, 075151 (2021).
[27] L. Fu, Topological Crystalline Insulators, Phys. Rev. Lett. **106**, 106802 (2011).
[28] T. H. Hsieh, H. Lin, J. Liu, W. Duan, A. Bansil, and L. Fu, Topological crystalline insulators in the snte material class, Nat. Commun. **3**, 982 (2012).
[29] H. Isobe and L. Fu, Theory of interacting topological crystalline insulators, Phys. Rev. B **92**, 081304(R) (2015).
[30] H. Song, S.-J. Huang, L. Fu, and M. Hermele, Topological Phases Protected by Point Group Symmetry, Phys. Rev. X **7**, 011020 (2017).
[31] S.-J. Huang, H. Song, Y.-P. Huang, and M. Hermele, Building crystalline topological phases from lower-dimensional states, Phys. Rev. B **96**, 205106 (2017).
[32] R. Thorngren and D. V. Else, Gauging Spatial Symmetries and the Classification of Topological Crystalline Phases, Phys. Rev. X **8**, 011040 (2018).

[33] L. Zou, Bulk characterization of topological crystalline insulators: Stability under interactions and relations to symmetry enriched $u(1)$ quantum spin liquids, Phys. Rev. B **97**, 045130 (2018).

[34] H. Song, C. Z. Xiong, and S.-J. Huang, Bosonic crystalline symmetry protected topological phases beyond the group cohomology proposal, Phys. Rev. B **101**, 165129 (2020).

[35] S. Jiang and Y. Ran, Anyon condensation and a generic tensor-network construction for symmetry-protected topological phases, Phys. Rev. B **95**, 125107 (2017).

[36] J. Kruthoff, J. de Boer, J. van Wezel, C. L. Kane, and R.-J. Slager, Topological Classification of Crystalline Insulators through Band Structure Combinatorics, Phys. Rev. X **7**, 041069 (2017).

[37] R.-J. Slager, A. Mesaros, V. Juričić, and J. Zaanen, The space group classification of topological band-insulators, Nat. Phys. **9**, 98 (2012).

[38] K. Shiozaki, M. Sato, and K. Gomi, Atiyah-hirzebruch spectral sequence in band topology: General formalism and topological invariants for 230 space groups, Phys. Rev. B **106**, 165103 (2022).

[39] Z. Song, S.-J. Huang, Y. Qi, C. Fang, and M. Hermele, Topological states from topological crystals, Sci. Adv. **5**, eaax2007 (2019).

[40] D. V. Else and R. Thorngren, Crystalline topological phases as defect networks, Phys. Rev. B **99**, 115116 (2019).

[41] Z. Song, C. Fang, and Y. Qi, Real-space recipes for general topological crystalline states, Nat. Commun. **11**, 4197 (2020).

[42] K. Shiozaki, C. Z. Xiong, and K. Gomi, Generalized homology and atiyah-hirzebruch spectral sequence in crystalline symmetry protected topological phenomena, arXiv:1810.00801.

[43] M. Cheng and C. Wang, Rotation symmetry-protected topological phases of fermions, Phys. Rev. B **105**, 195154 (2022).

[44] J.-H. Zhang, Q.-R. Wang, S. Yang, Y. Qi, and Z.-C. Gu, Construction and classification of point-group symmetry-protected topological phases in two-dimensional interacting fermionic systems, Phys. Rev. B **101**, 100501(R) (2020).

[45] A. Rasmussen and Y.-M. Lu, Classification and construction of higher-order symmetry protected topological phases of interacting bosons, Phys. Rev. B **101**, 085137 (2020).

[46] A. Rasmussen and Y.-M. Lu, Intrinsically interacting topological crystalline insulators and superconductors, arXiv:1810.12317.

[47] S.-J. Huang and M. Hermele, Surface field theories of point group symmetry protected topological phases, Phys. Rev. B **97**, 075145 (2018).

[48] S. Ono, H. C. Po, and K. Shiozaki, $\mathbb{Z}_2$-enriched symmetry indicators for topological superconductors in the 1651 magnetic space groups, Phys. Rev. Res. **3**, 023086 (2021).

[49] S.-J. Huang, 4d beyond-cohomology topologicalphase protected by c_2 symmetry and its boundary theories, Phys. Rev. Res. **2**, 033236 (2020).

[50] S.-J. Huang and Y.-T. Hsu, Faithful derivationof symmetry indicators: A case study for topological superconductors with time-reversal and inversion symmetries, Phys. Rev. Res. **3**, 013243 (2021).

[51] J.-H. Zhang, S. Yang, Y. Qi, and Z.-C. Gu, Real-space construction of crystalline topological superconductors and insulators in 2d interacting fermionic systems, Phys. Rev. Res. **4**, 033081 (2022).

[52] J.-H. Zhang and S. Yang, Tensor network representations of fermionic crystalline topological phases on two-dimensional lattices, arXiv:2109.06118.

[53] N. Manjunath and M. Barkeshli, Crystalline gauge fields and quantized discrete geometric response for abelian topological phases with lattice symmetry, Phys. Rev. Res. **3**, 013040 (2021).

[54] M. Barkeshli, Y.-A. Chen, P.-S. Hsin, and N. Manjunath, Classification of (2+1)d invertible fermionic topological phases with symmetry, Phys. Rev. B **105**, 235143 (2022).

[55] L. Fidkowski, A. Vishwanath, and M. A. Metlitski, Surface Topological Order and a new 't Hooft Anomaly of Interaction Enabled 3+1D Fermion SPTs, arXiv:1804.08628.

[56] M. Cheng, M. Zaletel, M. Barkeshli, A. Vishwanath, and P. Bonderson, Translational Symmetry and Microscopic Constraints on Symmetry-Enriched Topological Phases: A View from the Surface, Phys. Rev. X **6**, 041068 (2016).

[57] M. Cheng, Fermionic lieb-schultz-mattis theorems and weak symmetry-protected phases, Phys. Rev. B **99**, 075143 (2019).

[58] J. Sullivan and M. Cheng, Interacting edge states of fermionic symmetry-protected topological phases in two dimensions, SciPost Phys. **9**, 016 (2020).

[59] J.-H. Zhang and S.-Q. Ning, Crystalline equivalent boundary-bulk correspondence of two-dimensional topological phases, arXiv:2112.14567.

[60] J.-H. Zhang, Y. Qi, and Z.-C. Gu, Construction and classification of crystalline topological superconductor and insulators in three-dimensional interacting fermion systems, arXiv:2204.13558.

[61] Q. Wang, C.-C. Liu, Y.-M. Lu, and F. Zhang, High-Temperature Majorana Corner States, Phys. Rev. Lett. **121**, 186801 (2018).

[62] Z. Yan, F. Song, and Z. Wang, Majorana Corner Modes in a High-Temperature Platform, Phys. Rev. Lett. **121**, 096803 (2018).

[63] T. Liu, J. Jun He, and F. Nori, Majorana corner states in a two-dimensional magnetic topological insulator on a high-temperature superconductor, Phys. Rev. B **98**, 245413 (2018).

[64] Y. Wang, M. Lin, and T. L. Hughes, Weak-pairing higher order topological superconductors, Phys. Rev. B **98**, 165144 (2018).

[65] H. Shapourian, Y. Wang, and S. Ryu, Topological crystalline superconductivity and second-order topological superconductivity in nodal-loop materials, Phys. Rev. B **97**, 094508 (2018).

[66] R.-X. Zhang, W. S. Cole, and S. D. Sarma, Helical Hinge Majorana Modes in Iron-Based Superconductors, Phys. Rev. Lett. **122**, 187001 (2019).

[67] R.-X. Zhang, W. S. Cole, X. Wu, and S. Das Sarma, Higher-Order Topology and Nodal Topological Superconductivity in Fe(Se,Te) Heterostructures, Phys. Rev. Lett. **123**, 167001 (2019).

[68] R.-X. Zhang, F. Wu, and S. Das Sarma, Möbius insulator and Higher-Order Topology in $MnBi_{2n}Te_{3n+1}$, Phys. Rev. Lett. **124**, 136407 (2020).

[69] C.-H. Hsu, P. Stano, J. Klinovaja, and D. Loss, Majorana Kramers Pairs in Higher-Order Topological Insulators, Phys. Rev. Lett. **121**, 196801 (2018).

[70] N. Bultinck, B. A. Bernevig, and M. P. Zaletel, Three-dimensional superconductors with hybrid higher-order topology, Phys. Rev. B **99**, 125149 (2019).

[71] B. Roy, Higher-order topological superconductors in $\mathcal{P}$-, $\mathcal{T}$-odd quadrupolar dirac materials, Phys. Rev. B **101**, 220506(R) (2020).
[72] B. Roy and V. Juričić, Mixed-parity octupolar pairing and corner majorana modes in three dimensions, Phys. Rev. B **104**, L180503 (2021).
[73] K. Laubscher, D. Loss, and J. Klinovaja, Fractional topological superconductivity and parafermion corner states, Phys. Rev. Res. **1**, 032017(R) (2019).
[74] K. Laubscher, D. Loss, and J. Klinovaja, Majorana and parafermion corner states from two coupled sheets of bilayer graphene, Phys. Rev. Res. **2**, 013330 (2020).
[75] J.-H. Zhang, Strongly correlated crystalline higher-order topological phases in two-dimensional systems: A coupled-wire study, Phys. Rev. B **106**, L020503 (2022).
[76] J. May-Mann, Y. You, T. L. Hughes, and Z. Bi, Interaction enabled fractonic higher-order topological phases, Phys. Rev. B **105**, 245122 (2022).
[77] R.-X. Zhang, Bulk-vortex correspondence of higher-order topological superconductors, arXiv:2208.01652.
[78] A. K. Ghosh, T. Nag, and A. Saha, Hierarchy of higher-order topological superconductors in three dimensions, Phys. Rev. B **104**, 134508 (2021).
[79] J.-H. Zhang, M. Cheng, and Z. Bi, Classification and construction of interacting fractonic higher-order topological phases, Phys. Rev. B **108**, 045133 (2023).
[80] S.-B. Zhang, W. B. Rui, A. Calzona, S.-J. Choi, A. P. Schnyder, and B. Trauzettel, Topological and holonomic quantum computation based on second-order topological superconductors, Phys. Rev. Res. **2**, 043025 (2020).
[81] S.-B. Zhang, A. Calzona, and B. Trauzettel, All-electrically tunable networks of majorana bound states, Phys. Rev. B **102**, 100503(R) (2020).
[82] F. Tang, H. C. Po, A. Vishwanath, and X. Wan, Comprehensive search for topological materials using symmetry indicators, Nature (London) **566**, 486 (2019).
[83] H. C. Po, Symmetry indicators of band topology, J. Phys.: Condens. Matter **32**, 263001 (2020).
[84] E. Khalaf, H. C. Po, A. Vishwanath, and H. Watanabe, Symmetry Indicators and Anomalous Surface States of Topological Crystalline Insulators, Phys. Rev. X **8**, 031070 (2018).
[85] S. Ono and H. Watanabe, Unified understanding of symmetry indicators for all internal symmetry classes, Phys. Rev. B **98**, 115150 (2018).
[86] E. Lieb, T. Schultz, and D. Mattis, Two soluble models of an antiferromagnetic chain, Ann. Phys. (NY) **16**, 407 (1961).
[87] M. Oshikawa, Commensurability, Excitation Gap, and Topology in Quantum Many-Particle Systems on a Periodic Lattice, Phys. Rev. Lett. **84**, 1535 (2000).
[88] M. B. Hastings, Lieb-schultz-mattis in higher dimensions, Phys. Rev. B **69**, 104431 (2004).
[89] M. B Hastings, Sufficient conditions for topological order in insulators, Europhys. Lett. **70**, 824 (2005).
[90] B. Bradlyn, L. Elcoro, J. Cano, M. G. Vergniory, Z. Wang, C. Felser, M. I. Aroyo, and B. A. Bernevig, Topological quantum chemistry, Nature (London) **547**, 298 (2017).
[91] H. C. Po, H. Watanabe, C.-M. Jian, and M. P. Zaletel, Lattice Homotopy Constraints on Phases of Quantum Magnets, Phys. Rev. Lett. **119**, 127202 (2017).
[92] See Supplemental Material at http://link.aps.org/supplemental/10.1103/PhysRevB.108.L060504 for more details.
[93] N. Schuch, Condensed matter applications of entanglement theory, arXiv:1306.5551.